

Encapsulation of a Cu(II) complex with 2,6-pyridine dicarboxylic acid in zeolite-X nanoporosity as an efficient heterogeneous catalyst for oxidation of aniline

Fatemeh Hassani^a, Mahboubeh A. Sharif^{b*}, Masoumeh Tabatabaee^a, Mahboobeh Mahmoodi^c

a) Department of Chemistry, Yazd Branch, Islamic Azad University, Yazd, Iran

b) Department of Chemistry, Qom Branch, Islamic Azad University, Qom, Iran

c) Department of Biomedical Engineering, Yazd Branch, Islamic Azad University, Yazd, Iran

Received 30 March 2021; received in revised form 3 August 2021; accepted 7 August 2021

ABSTRACT

The Cu(II) complex of 2,6-pyridine dicarboxylic acid (PydcH₂, dipiconic acid) was successfully prepared and readily trapped in the nanocavity of zeolite-X (NaX) through a flexible synthetic method. The characterization of nanocomposite ([Cu(pydcH₂)(pydc)]-NaX) was performed by FT-IR, XRD, BET isotherm, SEM, TEM, and elemental analysis, that approved the encapsulating of coordination compound in the channels of NaX, with no change in the zeolite structure and morphology. The catalytic activity of the prepared material was also studied in respect of the oxidation of aniline with hydrogen peroxide as an oxidizing agent. The experiments were performed to optimize aniline oxidation under different extents of catalyst, temperature, and time. Optimized reaction conditions of this catalyst exhibited moderate activity (~92%) of aniline oxidation. This catalyst was stable in the oxidation of aniline as recovered and reused for an additional three runs. The outcomes reflected that the catalyst was reusable with no considerable loss in the catalytic activity.

Keywords: Zeolite-X; nanocomposite; nanoporosity, flexible ligand method; oxidation of aniline, dipicolinic acid

1. Introduction

Coordination compounds have good catalytic properties, and some of them are soluble in reaction solvents and act as homogeneous catalysts [1-3]. These homogenous catalysts indicate high selectivity and activity, but difficulty in product separation limit their industrial applications [4, 5]. Therefore, preparation of the heterogeneous catalysis was performed by some methods such as immobilization, grafting or encapsulation of homogeneous catalysis on the surface or in the cavities of inert solid (such as inorganic support or organic polymers) [6-10]. Zeolites are one of the best supporting materials due to having large unique framework structures, cavity topology, ion exchange properties, and thermal stability [11, 12]. The zeolite structure is entirely regular, with the construction segments formed in good order to create a 3-D framework with well-defined pores which show good stability in different areas and display high surface area [13].

Cages of the zeolites act like nanoreactors with proper molecular dimensions for encapsulating metal complexes [14-17]. The encapsulated complexes show the selectivity and reactivity of the same free form of complexes. Also, they have some benefits compared with homogenous catalysts, like superior stability, simple separation from the reaction mixture, and recyclability.

The zeolite synthesis methods such as template synthesis and flexible ligand are used to prepare zeolite encapsulated coordination compounds [18-20]. In this method, coordination compounds that were resistant under the zeolite synthesis condition (elevated pH and high temperatures) were encapsulated in zeolite cavities [21]. The flexible ligand method is one of the most extensively used methods for synthesizing zeolite encapsulated metal complexes [22-24]. In the flexible ligand system, the ligand size should be smaller than the dimensions of the zeolite channels. In this method, ion-exchanging of metal ions into zeolite should occur before entering the ligand to the zeolite cages. Once the

*Corresponding author:

E-mail address: m_sharif@qom-iaui.ac.ir (M. A. Sharif)

ligand enters the zeolite cage, it chelates with a metal ion to form a complex. The formed complexes are not able to exit from the zeolite cage because of their larger size than the zeolite pore diameter. In the template synthesis method, the ligand precursors diffuse into zeolite pores, and ligands are generated in the nanoporosity of zeolite. Ligands are coordinated with metals that are fixed by ion exchange, so these materials behave as a bicomponent catalyst or a bimetallic molecular sieve to modify the catalysis activity [25-29].

Aniline is a chemical used as a raw material widely used in producing the agrochemical, synthetic dyes, pharmaceuticals, explosives, plastics, drugs, rubber, herbicides, and photographic chemicals. Also it is often found in the environment *via* industrial wastewaters. [30]. Aniline in wastewater leads to environmental risks due to its high toxicity [31]. Therefore, efficient methods are required to remove this organic pollutant from water. This paper reports the synthesis and characterization of encapsulated Cu(II) coordination compound of pydcH₂ in the zeolite-X for the aniline oxidation.

2. Experimental

2.1. Materials and Physical methods of analysis

All chemicals were purchased from Sigma-Aldrich or Merck and used without further purification. FT-IR spectroscopy was documented through a Bruker Tensor 27 FT-IR-spectrophotometer (in the range between 400 and 4000 cm⁻¹, by KBr pellet). Field-emission scanning electron microscopy (FE-SEM) (TESCAN, Mira 3-XMU) and Transmission electron microscopy (TEM) (Zeiss-EM10C-80KV) were used to distinguish surface morphology and particle shape, respectively. X-ray diffraction (XRD) patterns were obtained from a

Philips, X'Pert PRO) by Cu K α radiation. The quantitative analysis of Si, Al, Na, and Cu(II) was performed by ICP-AES using PerkinElmer Optima 2000 DV. The GC (Gas Chromatography) analysis of samples was accomplished with an Agilent 6890N equipped with an HP-5 capillary column (30 m \times 0.32 mm ID \times 0.25 μ m film thickness) and a flame ionization detector (FID). Nitrogen adsorption measurements were calculated by a Sorptometer 1800 (Carlo-Erba instrument).

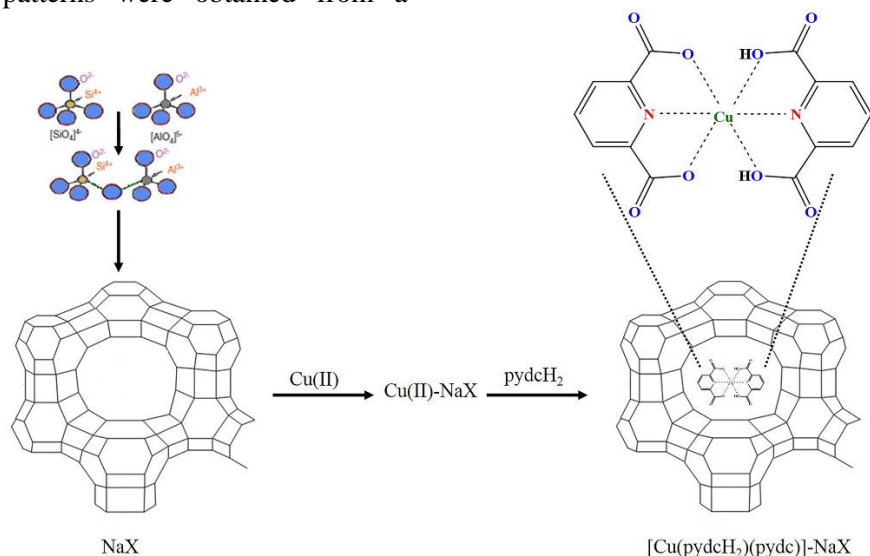
2.2. Catalyst preparation

2.2.1 Preparation of zeolite-X

X-type zeolite was synthesized from sodium silicate and sodium aluminate using a method reported in the literature [32]. Briefly, silica gel (3.0 g), sodium hydroxide (2.4 g) and deionized water (6 mL), were mixed in a plastic beaker to prepare sodium silicate (Na₂SiO₃) and stirred until all the materials dissolved. The sodium aluminate (NaAlO₂) solution was prepared simultaneously by adding sodium hydroxide (2.4 g), aluminum isopropoxide (6.9 g), and deionized water (9 mL) to a plastic beaker. Afterward, the NaAlO₂ and Na₂SiO₃ solutions and additional water (27 mL) were mixed and stirred until the mixture appeared homogenous. The mixture was rapidly transferred to a polypropylene bottle, sealed and located in an oven at about 90 °C.

2.2.2 Preparation of [Cu(pydcH₂)(pydc)]-NaX

The synthetic method of the encapsulated complex is presented in **Scheme 1**. The synthesis of zeolite encapsulated complex was carried out in two steps according to the general, flexible ligand method.



Scheme 1. Encapsulation of Cu(pydcH₂)(pydc)] complex in zeolite-X

2.2.2.1 Preparation of Cu(II) Exchanged Zeolite-X

Cu(II)-exchanged zeolite-X (Cu(II)-NaX), was prepared based on the procedure described in the literature [33]. Zeolite-X (4.0 g) was suspended in a 250 mL solution of $\text{Cu}(\text{NO}_3)_2 \cdot 6\text{H}_2\text{O}$ (1.183 g, 4.0 mmol) and refluxed at 90 °C for 24 h. The solid was filtered and the residue was washed by a great volume of warm deionized water to remove excess copper ions. The resulting residue was dried at 150 °C for 15 h.

2.2.2.2 Preparation of Encapsulated Cu(II) Complex in NaX

A mixture of Cu(II)-NaX (1.0 g) and pydcH_2 (12.0 mmol) in ethanol (100 mL) was refluxed and stirred in an oil bath overnight. The resulting residue was subject to Soxhlet extraction in acetonitrile and ethanol for two h (to remove the additional unreacted ligand in the channels of the zeolite and any free Cu(II) complex located on the surface of the zeolite). The resulting residue was filtrated off and was dried at 120 °C for 20 h. The dried residue was suspended in 100 mL of 0.01 M NaOH solution for 24 h to remove excess unreacted Cu(II) ions. Finally, the filtrated residue was dried at 120 °C.

2.3 Catalytic Reaction for the oxidation of aniline

A mixture of aniline (2 mL), acetonitrile (4 mL, as a solvent), hydrogen peroxide (2 mL, 30 wt.%, as an oxidant), and different amounts of catalyst was stirred and refluxed (for 2.0 h, at 30°C). Then, to recover the catalyst, the residue was filtrated and washed with solvents for reuse. The filtrate was collected, centrifuged, then the supernatant solution of the reaction mixture was mixed with 0.2 mL of Dioxane as internal standard. Finally, the mixture was subject to GC analysis.

3. Result and Discussion

The silica and alumina present a soluble sodium aluminosilicate when treating with sodium hydroxide solution. The preparation of zeolite is significantly related to the PH (alkali medium), and the temperature applied. The crystallization process of zeolite occurs *via* nucleation of aluminosilicate ions and crystal growth.

3.1 Characterization of encapsulated Cu(II) complex in zeolite-X

3.1.1 FT-IR spectroscopy

The FT-IR spectra of the prepared NaX and its encapsulated Cu complex are shown in **Fig. 1**. The absorption bands of IR spectrum concerning zeolites are observed as two parts of vibrations: (a) internal

vibrations of AlO_4 and SiO_4 tetrahedral fragments, which are insensible to the structural vibrations, and (b) the external vibrations of the AlO_4 and SiO_4 units which are sensitive to the structural linkages. The intense band at 987 cm^{-1} is related to an asymmetric stretching of Si-O-Al [34,35]. The fundamental framework vibration of SiO_4 and AlO_4 groups are seen in the mid-infrared region of the spectrum by the band at 1101 cm^{-1} . The weak band at 3342 cm^{-1} is related to the stretching vibrations of the O-H group, indicating the hydrated aluminum silicates form. The bending mode of water molecules was observed in bands at 1625 cm^{-1} and 1392 cm^{-1} [36,37]. Therefore, the formation of NaX was confirmed by the above information.

The formation of the Cu(II) complex in the nanoporosity of NaX is confirmed by the extra bands in comparison with FT-IR spectroscopy of parent NaX. The coordination of Cu(II) was approved by the bands around the 3400 cm^{-1} area (related to the connections of the OH groups from dipicolinate). The vibration around 1648 cm^{-1} is related to the C=O stretching frequency of the carboxylate groups [38]. This band was shifted to a lower wave number, compared with pydcH_2 ($1710\text{--}1739\text{ cm}^{-1}$), because of the coordination of the -COO group to the Cu(II) ion. The band at 1384 cm^{-1} is related to the C-O stretching frequency in pydcH_2 [39]. The intense band at 968 cm^{-1} was devoted to an asymmetric stretching of Si-O-Al for Na-X, combined with the C-C and C=C stretching of pydcH_2 , confirmed by the band's broadening [40, 41]. No shift or expansion of zeolite vibrations is considered upon the incorporation of the coordination compounds, which gives significant confirmation. The zeolite framework stays with no change.

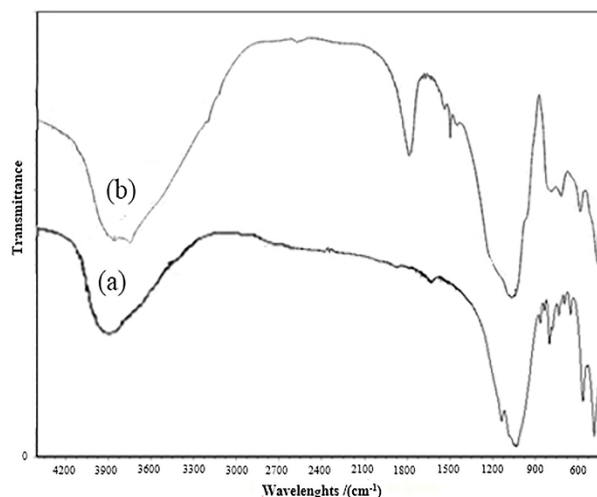


Fig. 1 FTIR spectra of (a) NaX, and (b) $[\text{Cu}(\text{pydcH}_2)(\text{pydc})\text{-NaX}$

3.1.2 Analytical data

Table 1 contains the data analytics of host NaX, Cu(II)-NaX and ([Cu(pydcH₂)(pydc)]-NaX nanocomposite. The Si/Al molar ratio of NaX is 1.22, which is in agreement with the unit cell formula Na₈₈Al₈₈Si₁₀₄O₃₈₄ [42]. The Si/Al ratio stayed with no change in Cu(II)-NaX, which supported no dealumination with ion exchange. The C/N ratio in [Cu(pydcH₂)(pydc)]-NaX exhibited just slight distortion (compared to the free complex), which affirmed the structure of the complex has been unchanged in the channels of zeolite. The Cu, C, H, and N contents display a ligand/metal ratio of around 2:1 for the [Cu(pydcH₂)(pydc)]-NaX. However, a little lower molar ratio in each case demonstrates minute traces of free metal ions in the latticework.

3.1.3 powder X-ray diffraction

XRD patterns of NaX, Cu(II) exchanging zeolite-X and ([Cu(pydcH₂)(pydc)]-NaX) were obtained at $2\theta = 0^\circ - 70^\circ$ (**Fig. 2**). All have a main peak at 2θ value of 26.61 and XRD measurement displays that the loading of the Cu(II) complex of pydcH₂ in the pores of zeolite-X exhibits no intense effects in the framework of the zeolitic matrix that stands intact [43]. Loading of the complex in the structural framework of zeolite X leads to the minor changes in XRD patterns and in the intensity of the peaks, which is reflected in the change in the position of the peaks, too. [44-46].

3.1.4 BET-Surface area

The surface area specification of the [Cu(pydcH₂)(pydc)]-NaX was investigated by N₂ sorption at 77 K (**Fig. 3**). Based on IUPAC systematization, the isotherm of [Cu(pydcH₂)(pydc)]-NaX was type I, which was in agreement with the previous report on nitrogen sorption isotherm data of NaX [47]. Although these indicated the microporous nature of the material [48], tiny increased amount of nitrogen at P/P0 values larger than 0.9 affirmed the existence of a low quantity of macropores (pore diameters of more than 50nm). In addition, a slender hysteresis loop was generally observed for the [Cu(pydcH₂)(pydc)]-NaX, that was specification of the substances containing both micropores and mesopores (**Fig. 3a**) [49]. The range of linearity of the BET plot was only from 0.02 to 0.2. In addition, the catalyst indicates a slender BJH pore size distribution curve as shown in **Fig. 3b** [50].

BET surface area (SBET) and total pore volume (V_p) of the NaX and encapsulated complex are given in **Table 2**. The surface area and pore volume of the [Cu(pydcH₂)(pydc)]-NaX exhibited a noticeable decrease in comparison to parent NaX. According to the FTIR spectrum and XRD pattern the crystal structure of the NaX wasn't changed by the load of complex, because the complexation was performed in the NaX supercages instead of the external surface.

Table 1 Analytical data for NaX, Cu(II)-NaX and ([Cu(pydcH₂)(pydc)]-NaX

Compound	%Cu	%C	%N	%H	C/N	%Si	%Al	%Na	Si/Al
Na-X	-	-	-	-	-	20.55	16.84	16.92	1.22
Cu-Na-X	4.12	-	-	-	-	20.92	17.14	6.3	1.22
Cu-L-NaX	2.83	7.43	1.24	0.38	5.99	20.57	16.86	7.6	1.22

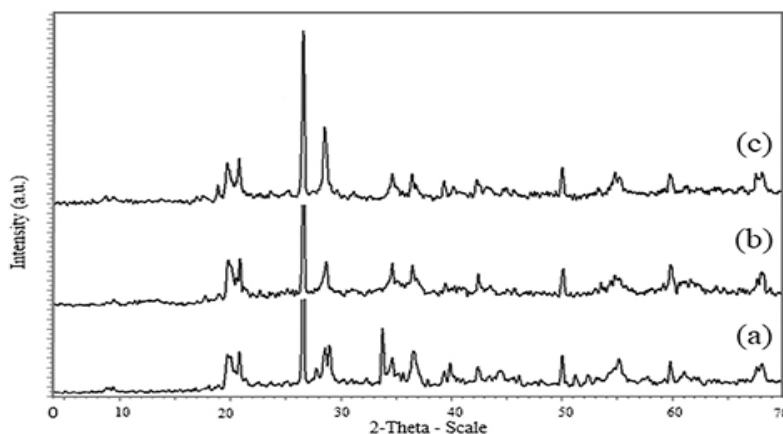


Fig. 2. XRD patterns of (a) NaX, (b) Cu-NaX and (c) [Cu(pydcH₂)(pydc)]-NaX

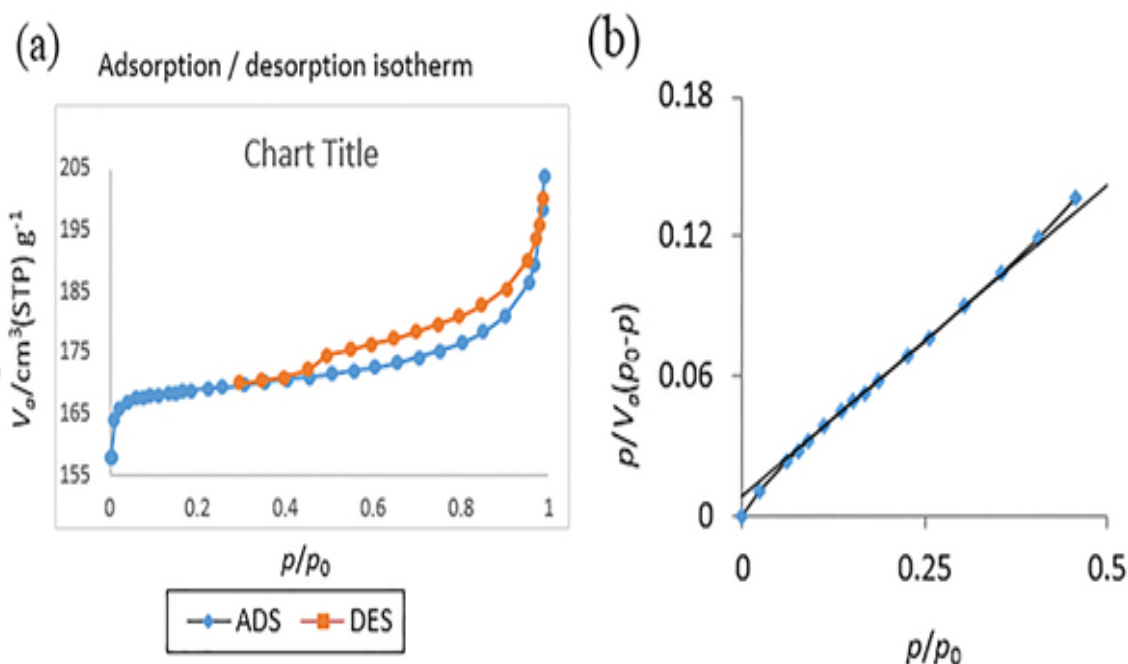


Fig. 3. (a) Nitrogen adsorption–desorption isotherms, (b) BET plot of [Cu(pydcH₂)(pydc)]-NaX

Table 2 Some surface characteristics data of NaX and [Cu(pydcH₂)(pydc)]-NaX

Sample	S _{BET} (m ² /g)	V _p (cm ³ /g)
NaX	620.089	0.255972
[Cu(pydcH ₂)(pydc)]-NaX	601.736	0.188499

3.1.5 Scanning /Transmission electron microscopy

The scanning electron microscopy (SEM) images of the NaX and [Cu(pydcH₂)(pydc)]-NaX are shown in **Fig. 4**. SEM image of the [Cu(pydcH₂)(pydc)]-NaX indicate the presence of well-defined zeolite crystals without any effect of Cu(II) ions or complex present on its external surface. The notable difference in SEM image of the zeolite and the zeolite encapsulated Cu (II) complex is an evidence for the encapsulation of Cu (II) complex. The aggregation of rough spheres of undefined shape confirms the formation of zeolite-X [51-53]. A uniform orientation and morphology can be observed by single-phase formation.

The TEM photographs of the NaX and [Cu(pydcH₂)(pydc)]-NaX are shown in **Fig. 5**. These exhibit that the structure of both are rectangular, cubic and that their channels are well arranged. The [Cu(pydcH₂)(pydc)]-NaX also displays an opaque

character and well-arranged form but with a little change at the surface margins. Furthermore, partial agglomeration is considered as compared to parent zeolite. Because of the encapsulation of complex segments in the channels of the zeolite, the morphology of the [Cu(pydcH₂)(pydc)]-NaX shows crystalline nature. The picture of [Cu(pydcH₂)(pydc)]-NaX shows the lack of Cu(II) complex traces on the surface.

1.2 Catalytic activity (Oxidation of aniline)

The catalytic activity of the [Cu(pydcH₂)(pydc)]-NaX was carried out by the oxidation of aniline (2 mL) in the presence of acetonitrile (4 mL), H₂O₂ (2 mL) and Dioxane (0.2 mL) to its insoluble nitroso benzene. In order to optimize the process, the batch experiments were carried out under different contact times (60, 90, 120, 150 and 180 min), temperature (30, 45 and 60 °C) and catalyst amount (6, 7, 8, 9, 10, 11 and 12 mg) and holding all other factors constant (**Table 3**).

The aniline oxidation was carried out in the various states and the aniline concentration was defined by a GC analysis using the measure of residual concentrations. The removal yield, R (%) was computed using the following formula [54]:

$$R = \frac{(C_0 - C_t)}{C_0} * 100$$

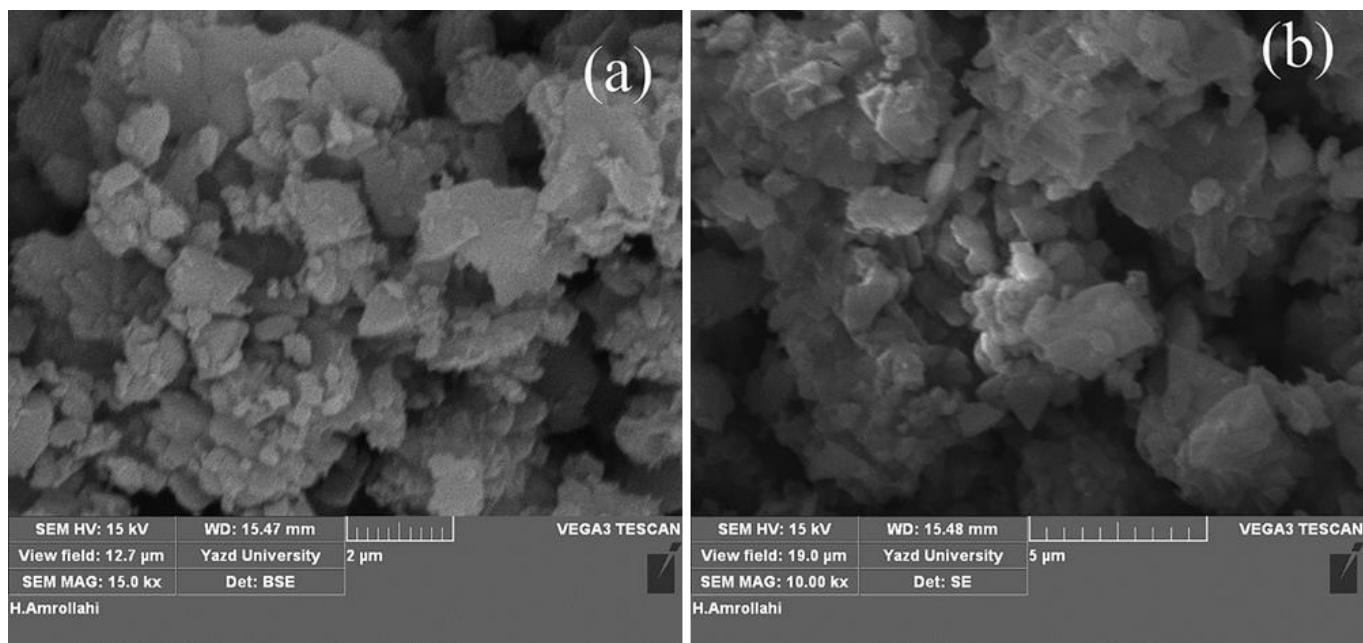


Fig. 4 SEM images of the (a) NaX, (b) [Cu(pydcH₂)(pydc)]-NaX

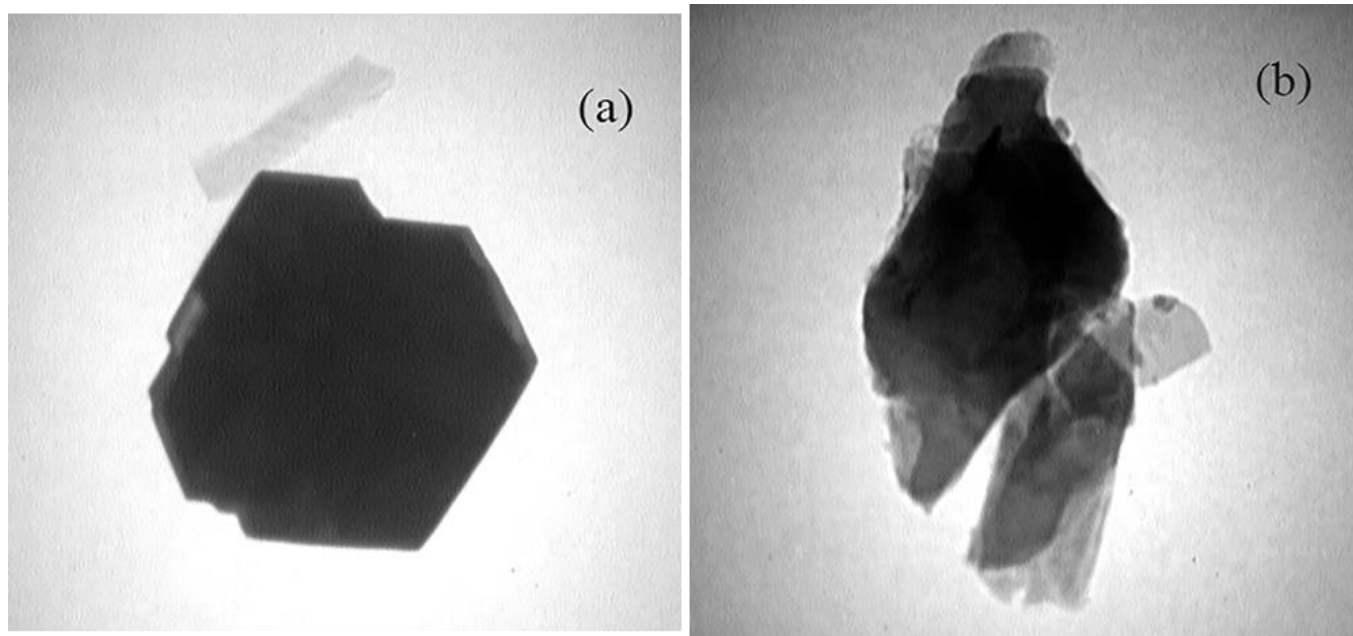


Fig. 5. TEM images of the (a) NaX, and (b) [Cu(pydcH₂)(pydc)]-NaX

Where C_0 and C_t indicate the initiatory and terminal of aniline concentrations (after the removal process), respectively.

As expected, the results indicated that a higher temperature and time could accelerate degradation, which were in accordance with the former reports [55-57].

To find the optimum amount of catalyst, the aniline oxidation was performed at different amounts of catalyst from 6 mg to 13 mg. The 90.15% of oxidation efficiency

was gained during 2 h of reaction at 30 °C with 10 mg of catalyst (**Table 3**). The oxidation of aniline to niroso elevates with enhancement in amount of catalyst up to 10 mg but additional rise in catalyst amount over the optimized quantity exhibited decrease in aniline oxidation yield because of reduction in the access of active sites. The extra value of catalyst stands to H₂O₂ decomposition that will finally prevent the reaction [58].

Since the pure coordination compounds cannot be recycled even once, they lost their catalytic activity after use. However, the heterogenous catalyst could be reused

Table 3 Effect of various parameters on the reactivity

Row	Amount of catalyst (mg)	T (°C)	Time (min)	Conver. (%)
1	0	30	120	24.61
2	6	30	120	57.83
3	7	30	120	67.62
4	8	30	120	74.21
5	9	30	120	83.72
6	10 ^a	30	120	90.15
7	10 ^b	30	120	86.91
8	10 ^c	30	120	85.13
9	11	30	120	87.18
10	12	30	120	85.12
11	13	30	120	80.61
12	10	30	120	90.15
13	10	45	120	92.14
14	10	60	120	93.84
15	10	90	120	96.54
16	10	30	60	71.89
17	10	30	90	84.89
18	10	30	120	90.15
19	10	30	150	94.66
20	10	30	180	97.74

Reaction condition: H₂O₂: 2 mL; aniline: 2 mL; acetonitrile: 4 mL.

^a First reuse, ^b Second reuse, ^c Third reuse.

after filtering and washing without significant damage in catalytic activity [59]. The catalyst was reused under same situations after the completion of the reaction, filtration and separation of the catalyst and washed with solvent. The result by atomic absorption spectroscopy exhibited no loss in the amount of copper, they showed a little loss in catalytic activity. To investigate the catalyst effect, aniline oxidation was performed by H₂O₂ without catalyst. The result of this experiment showed that H₂O₂ (without catalyst) could oxidize less than 25 % of anilines.

Aniline oxidation using several heteropolyanions was studied by Alizadeh *et al.* [60]. Their report showed that nitrosobenzene and nitrobenzene were the main and minor products for catalytic aniline oxidation, respectively. Their report exhibited that yield of aniline oxidation in the presence of H₃PW₁₂O₄₀, was just 55 %

while conversion to nitrobenzene was performed only 8.5 % (after 15 min).

4. Conclusions

The flexible ligand method was used to encapsulate a Cu(II) complex in the NaX and was used as a catalyst for the oxidation of aniline in different conditions. The best yield was obtained during the oxidation of aniline using 10 mg of the catalyst with 2 mL of H₂O₂ at 30°C after 2h. Furthermore, the result showed the encapsulated Cu(II) coordination compound could be recovered and reused with no loss of activity.

Acknowledgements

We express our gratefulness to Yazd branch, Islamic Azad University for preparing the required laboratory facilities and financial support.

References

- [1]. S. Zhang, Q. Fan, R. Xia, T.J. Meyer, *Acc. Chem. Res.* 53 (2020) 255–264
- [2]. E. Larsen, K.A. Jørgensen, *Acta Chem. Scand.* 43 (1989) 259–263
- [3]. A. Arora, S. Singh, P. Oswal, D. Nautiyal, G.K.Rao, S. Kumar, A. Kumar, *Coord. Chem. Rev.* 438 (2021) 213885–213899
- [4]. N.D. Knçfel, H. Rothfuss, J. Willenbacher, C. Barner-Kowollik, P.W. Roesky, *Angew. Chem. Int. Ed.* 56 (2017) 4950–4954
- [5]. V.S. Shende, V.B. Saptal, B.M. Bhanage, *Chem. Rec.* 19 (2019) 1–23
- [6]. S. Kumari, S. Ray, *New J. Chem.* 44 (2020) 44, 14953–14963
- [7]. R. Bera, C. Adhikary, *J. P. Mat.* 28 (2021) 695–702
- [8]. I. Chorkendorff, J.W. Niemantsverdriet, *Concept of modern catalysis and kinetics*, Wiley-VCH GmbH & Co. KGaA, Weinheim, Germany, 2003
- [9]. A. Dergunov, A.T. Khabiyev, S.N. Shmakov, M.D. Kim, N. Ehterami, *ACS Nano*, 10 (2016) 11397–11406
- [10]. P. Eghbali, E. Şahin, M. Masteri-Farahani, *J. Porous Mat.* 24 (2017) 39–44
- [11]. R. Abraham, K.K.M. Yusuff, *J. Mol. Catal. A: Chem.* 198 (2003) 175–183
- [12]. C. Jin, W. Fan, Y. Jia, B. Fan, J. Ma and R. Li, *J. Mol. Catal. A: Chem.*, 249 (2006) 23–30.
- [13]. A. Primo and H. Garcia, *Chem. Soc. Rev.*, 43 (2014) 7548–7561.
- [14]. A.P. Sameeha, M. Sebastian, P.M.S. Begum, K.K.M. Yusuff, *Chem. Data Collect.* 26 (2020) 100351–52
- [15]. F. Li, D. Hu, Y. Yuan, B. Luo, Y. Song, S. Xiao, G. Chen, Y. Fang, F. Lu, *Mol. Catal.* 452 (2018) 75–82

- [16]. K.S. Ambili, J. Thomas, J. Porous Mat. 27 (2020) 755-764
- [17]. A.H. Ahmed, M.S. Thabet, J. Mol. Struct. 1006 (2011) 527-535
- [18]. S. Rayati, N. Rafiee, F. Nejabat, Inorg. Chem. Res. 4 (2020) 86-93
- [19]. B.P. Nethravathi, J. Porous Mat. 23 (2016) 1305-1310
- [20]. M.R. Maurya, A.K. Chandrakar, S.H. Chand, J. Mol. Catal. A Chem. 263 (2007) 227-237
- [21]. L.G. Qiu, A.J. Xie, L.D. Zhang, Adv. Mater. 17 (2005) 689-692
- [22]. A.A. Varghese, K.K.M. Yusuff, Mater. Today, 25 (2020) 186-191
- [23]. M. Sharma, B. Das, A. Hazarika, N.S.V.M. Rao Mangina, G.V.Karunakar, K.K. Bania, Micropor. Mesopor. Mat. 272 (2018) 31-39
- [24]. J. Kenneth, J.R. Balkus, A.A. Welch, B.E. Gnade, Zeolites 10 (1990) 722-729
- [25]. H. Wang, L. Wang, F.S. Xiao, ACS Cent. Sci. 6 (2020) 1685-1697
- [26]. X. Yuan, F. Li, L. Wang, H.A. Luo, Latin Am. Appl. Res. 37 (2007) 151-156
- [27]. M. Salavati-Niasari, J. Incl. Phenom Macro. Chem. 65 (2009) 317-328
- [28]. R. Ferreira, M. Silva, C. Freire, B. Castro, J.L. Figueiredo, Microporous Mesoporous Mater. 38 (2000) 391-401
- [29]. J. Yu, Z. Zhen, Q. Ding, Y. Zhang, X. Wu, L. Sun, J. Du, Catal. Today, 339 (2020) 105-112
- [30]. A. Benito, A. Penades, J.L. Lliberia, R. Gonzalez-Olmos, Chemosphere 166 (2017) 230-237
- [31]. X. Li, Shao D, H. Xu H, L. Wei, Y. Wei, Chem Eng J. 285 (2016) 1-10
- [32]. K.J. Balkus, K.T. Ly, J. Chem. Educ. 68 (1991) 875-877
- [33]. C.K. Modi, P.M. Trivedi, Adv. Mat. Lett. 3 (2012) 149-153
- [34]. M. Davidova, D. Nachtigallova, R. Bulanek, P. Nachtigall, J. Phys. Chem. B 107 (2003) 2327-2332
- [35]. N. Gupta, A.K. Kushwaha, M.C. Chattopadhyaya, Adv. Mat. Lett. 2 (2011) 309-312
- [36]. A.G. Charles, Eur. J. Mineral. 24 (2012) 439-445
- [37]. M. Ramalingam, N. Sundaraganesan, H. Saleem, J. Swaminathan, Spectrochim. Acta A Mol. Biomol. Spectrosc. 71 (2008) 23-30
- [38]. S. Priyanka, N.P. Singh, R.A. Yadav, J. Chem. Pharm. Res. 2 (2010) 656-681
- [39]. H. Aghabozorg, F. Ramezanipour, J. Soleimannejad, M.A. Sharif, A. Shokrollahi, M. Shamsipur, A. Moghimi, J. Attar Gharamaleki, V. Lippolis, A.J. Blake, Polish J. Chem. 82 (2008) 487-507
- [40]. D.H. Robert, A.T. David, Inorg. Nucl. Chem. Lett. 3 (1967) 419-422
- [41]. R.A. Yadav, M. Kumar, R. Singh, S. Priyanka, N.P. Singh, Spectrochim. Acta Part A 84 (2011) 6-21
- [42]. S. Golbad, P. Khoshnoud, G. Keleney, N. Abu-Zahra, Water Environ. J. 34 (2019) 342-349
- [43]. J. Scott, D. Guang, K. Naeramitarnasuk, M. Thabuot, R. Amal, J. Chem. Technol. Biotechnol., 77 (2001) 63-69
- [44]. C.K. Modi, M.T. Parthiv, Adv. Mat. Lett. 3 (2012) 149-153
- [45]. A. Kozlov, K. Asakura, Y. Iwasawa, J. Chem. Soc. Faraday Trans. 94 (1998) 809-816
- [46]. S.A. Chavan, D. Srinivas, P. Ratnasamy, Chem. Commun. 12 (2001) 1124-1125
- [47]. M. Anbia, F. Mohammadi Nejati, M. Jahangiri, A. Eskandari, V. Garshasbi, J. Sci. I.R.I. 26 (2015) 213-222
- [48]. H. Naeimi, M. Moradian, Appl. Catal. A 467 (2013) 400-406
- [49]. A. Mohammadi Zardkhouhoui, S.S. Hosseiny Davarani, Nanoscale 12 (2020) 12476-12489
- [50]. H.S. Abbo, S.J. Titinchi, Top Catal. 53 (2010) 1401-1410
- [51]. H. Mimura, K. Yokota, K. Akiba, Y. Onodera, J. Nucl. Sci. Technol. 38 (2001) 766-772
- [52]. C. Belviso, F. Cavalcante, S. Fiore, Waste Manage. 30 (2010) 839-847
- [53]. P. Pengthamkeerati, T. Satapanajaru, P. Chularuengsoarn, Fuel 87 (2008) 2469-2476
- [54]. S. Ahmadi, C.A. Igwegbe, Appl. Water Sci. 8 (2018) 170, 1-8
- [55]. Y.Z. Zhan, H.L. Li, Y.L. Chen, J. Hazard. Mater. 180 (2010) 481-485
- [56]. J. Qian, K. Wang, Q. Guan, H. Li, H. Xu, Q. Liu, W. Liu, B. Qiu, Appl. Surf. Sci. 288 (2014) 633-640
- [57]. V. Huleaa, E. Dumitriu, Appl. Catal. A-Gen. 277 (2004) 99-106
- [58]. I. Ambat, V. Srivastava, E. Haapaniemi, M. Sillanpaa, Renew. Energ. 139 (2019) 1428-1436
- [59]. M. Tabatabaee, S. Hashemian, M. Roozbeh, M. Roozbeh, M. Mirjalili, Res. Chem. Intermed. 41 (2015) 231-234
- [60]. M.H. Alizadeh, R. Tayebee, J. Braz. Chem. Soc. 16 (2005) 108-111.